Polymer Chemistry

Crystallization and Self-assembly of Shape-Complementary Sequence-defined Peptoids

Journal:	*Polymer Chemistry*
Manuscript ID	PY-ART-03-2021-000426.R1
Article Type:	Paper
Date Submitted by the Author:	26-May-2021
Complete List of Authors:	Xuan, Sunting; Soochow University Jiang, Xi; E O Lawrence Berkeley National Laboratory, Materials Sciences Division Balsara, Nitash; University of California Berkeley, Chemical and Biomolecular Engineering Zuckermann, Ronald; Lawrence Berkeley National Laboratory, Biological Nanostructures Facility

Crystallization and Self-assembly of Shape-Complementary Sequence-defined Peptoids

Sunting Xuan,[a,b,d] Xi Jiang,[a] Nitash P. Balsara,[a,c] and Ronald N. Zuckermann*[a,b]

[a] Materials Sciences Division, Lawrence Berkeley National Laboratory, Berkeley, CA 94720 United States.

[b] Molecular Foundry, Lawrence Berkeley National Laboratory, Berkeley, CA 94720 United States.

[c] College of Chemistry, University of California, Berkeley, Berkeley, CA 94720 United States.

[d] College of Chemistry, Chemical Engineering and Material Science, Soochow University, Suzhou, Jiangsu, China, 215123

Abstract

The universal pairing of complementary nucleobases in DNA found in all life forms has inspired extensive studies on selective molecular recognition between information-rich sequence-defined polymer chains. Here we utilized the shape complementarity of sequence-defined peptoids to achieve selective assembly between peptoid chains. Three sets of self-complementary peptoids bearing different overall molecular shapes-determined by the monomer sequence (trapezoid, comb and zig-zag)-were synthesized and systematically studied by differential scanning calorimetry and X-ray diffraction. All these peptoids crystallized in bulk into a nearly identical rectangular crystal lattice as evidenced by their similar melting temperatures and X-ray diffraction peaks. In aqueous solution, they all self-assembled into crystalline monolayer nanosheets with a known rectangular crystal lattice motif, regardless of their varied molecular shapes. These results suggest that complementary molecular shape could be a potential design element for the construction of more sophisticated, hierarchically-ordered peptoid nanomaterials that approach the structural and functional complexity found in biomacromolecular nanostructure.

Introduction

DNA is a crucial macromolecule carrying genetic information essential for all known forms of life. The specific recognition of complementary polynucleotide single strands *via* Watson-Crick base pairing is at the foundation of DNA transcription and replication.[1] Inspired by the precise structure of the DNA double-helix and its high chemical information content, chemists have long sought to mimic some of these attributes in simpler polymer systems. A common approach is to incorporate complementary hydrogen-bonding moieties to polymer backbones to guide the intermolecular recognition between polymer chains.[2-4]

Although hydrogen bonding is one of the key determinants of specificity in Watson-Crick base pairing, shape complementary also plays a major role, and is at the root of many biomolecular interaction in enzyme function, antibody recognition and host-guest interaction.[5-6] Studies have successfully utilized shape complementarity for the construction of intricate supramolecular nanostructures made from biomolecules (e.g., DNA origami) and synthetic molecules (e.g., nanoparticles).[7-11] However, the study of inter-chain molecular recognition of synthetic polymers based on shape complementarity is still at a very early stage.

Precise control over the sequence of chemically distinct monomers within a polymer chain is the prerequisite to achieve the assembly of complex and hierarchical nanostructures through specific molecular recognition as found in DNA and proteins. Poly(*N*-substituted glycines) (a.k.a. polypeptoids), a class of non-natural sequence-defined polymers, have emerged as a desirable building block to create ordered biomimetic nanostructures.[12-15] The efficient and iterative submonomer solid-phase synthesis of peptoids, using primary amines as synthons, allows the incorporation of chemically diverse side chains at specific position along the backbones to obtain precisely controlled sequences.[16] The peptoid platform has been used to study inter-chain

recognition. For example, the Scott group successfully demonstrated the hetero-recognition of two different sequence-defined peptoid chains *via* dynamic covalent bonding.[17-18] They designed two complementary sequence-defined peptoids, one with amine-based side chains and the other with aldehyde-based side chains, which can undergo sequence-selective condensation in solution by dynamic covalent chemistry between amine and aldehyde groups, to afford in-registry molecular ladders with imine-based covalent rungs.[17] They also demonstrated the temperature-mediated assembly of sequence-defined peptoids containing maleimide and furan side groups to obtain molecular ladders with Diels-Alder adduct based rungs.[18]

Because a specific sidechain can be chosen for every position in the sequence, peptoids offer the opportunity to precisely control the overall molecular shape, and explore its impact on chain-chain recognition. Lacking hydrogen bond donors in the backbone, the impact of peptoid shape can be probed in the absence of other interfering interactions. Linear and cyclic peptoids with *n*-alkyl side chains have been shown to be crystalline in bulk.[19-21] Our previous work showed that the highly crystalline linear peptoids bearing *n*-alkyl side chains prefer to adopt a planar board-like crystal lattice with extended backbone conformations.[19-20] Importantly, we have also shown that in many cases the side chains of these peptoids can be altered without changing the backbone conformation in the crystal lattice.[22] In a sense this is reminiscent of the way DNA strands bind to one another: the backbones adopt the same fold regardless of sequence, and the recognition takes place between the side chains. Thus, peptoids provide the opportunity to explore shape-complementary between parallel (or anti-parallel) *N*-alkyl peptoid chains.

Here, for the first time, we explore the selective assembly of sequence-defined amphiphilic diblock copolypeptoids, poly(*N*-alkylglycine)-*b*-poly(*N*-2-(2-methoxyethoxy)ethylglycine), with self-complementary hydrophobic domain shapes in bulk and solution. In contrast to the dynamic

covalent chemistry of Scott mentioned above[17], the predominant van der Waals interactions between peptoid chains in our study are much weaker. We expect, however, the cumulative interaction effect to be significant since the interfacial contact area is considerably larger in a crystal lattice as compared to the solution interaction of only two molecules. Three sets of peptoids bearing different molecular shapes of the hydrophobic block (trapezoid, comb and zig-zag), as shown in Figure 1, were synthesized and purified by HPLC. We anticipated that the adjacent rows of peptoids in the side chain to side chain direction (the *c* direction) to be oriented in an antiparallel manner.[19-20, 23-24] The main chain length for all the peptoids was kept the same, while the side chain length was varied from heptyl to decyl in such a way to keep the inter-backbone distance constant in the *c* direction assuming a rectangular crystal lattice as previously reported.[19-20, 23-24] The peptoids were systematically studied by differential scanning calorimetry (DSC) and X-ray diffraction. All peptoids exhibited a similar melting temperature and a similar X-ray diffraction pattern in bulk, revealing their crystallization into a nearly identical rectangular crystal lattice. Despite their different molecular shapes, the peptoids with self-complementary shapes all self-assembled, through inter-strand recognition, into crystalline nanosheets with similar rectangular crystal lattices. This study demonstrated the successful utilization of self-complementary molecular shapes of peptoids in directing their self-assembly in bulk and solution. Similar to the information-directed hybridization of complementary nucleic acid sequences, the complementary molecular shape holds the potential as a design element for the creation of more complex and hierarchical peptoids nanostructures resembling the structural and functional complexity found in nature.

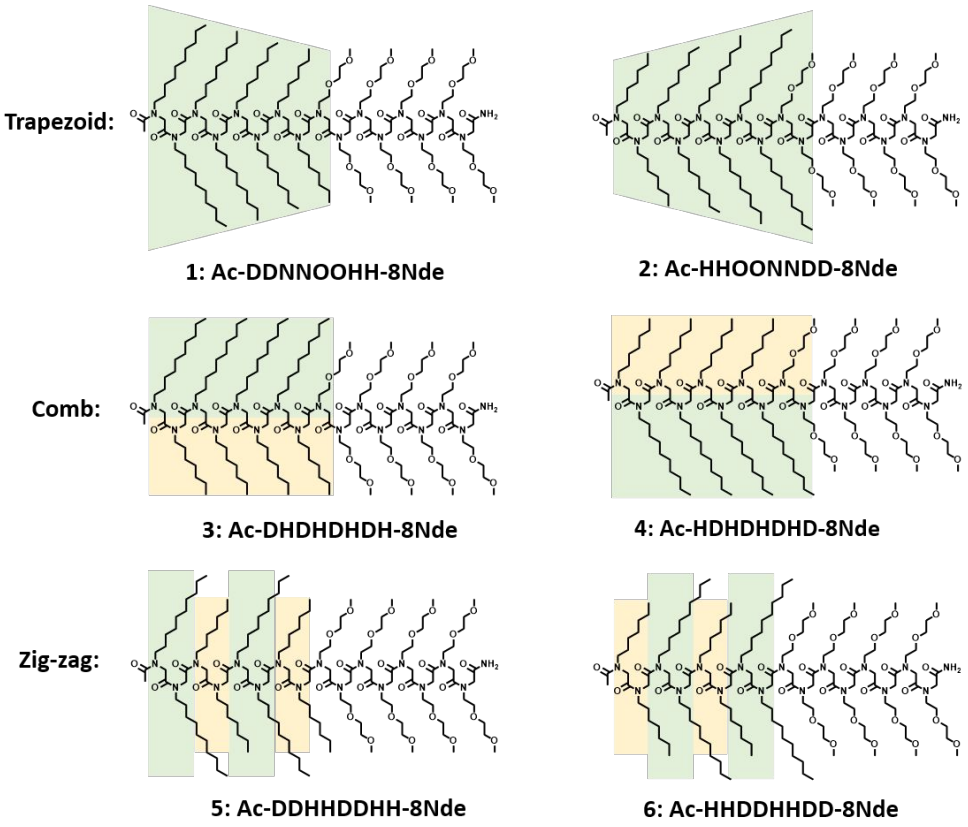

Figure 1. Chemical structures of diblock copolypeptoids bearing a same hydrophilic Nde block and a hydrophobic block of different shape. *N*-decyl glycine is denoted as **D** and *N*-heptyl glycine is denoted as **H**. The side chain length of the hydrophobic block was kept constant while the position was arranged differently. The green and yellow colors indicated the different shapes of molecules.

Experimental Section

Synthesis of Diblock Copolypeptoids. The 2-(2-methoxyethoxy)ethylamine, decylamine, nonylamine, octylamine, heptylamine, bromoacetic acid, trifluoroacetic acid (TFA), pyridine and acetic anhydride were purchased from Sigma Aldrich. *N,N'*-diisopropylcarbodiimide (DIC) was purchased from Chem-Impex. 4-Methylpiperidine was purchased from TCI. Rink amide resin was purchased from Novabiochem. All the solvents and reagents used in the study were directly used as received. All diblock copolypeptoids were synthesized by automated submonomer solid-phase synthesis on a Symphony X peptide synthesizer at a scale of 200 mg Rink amide resin

with 0.64 mmol/g loading efficiency using adapted procedures. The resin was first swelled in dimethylformamide (DMF) for 10 min followed by deprotection of the Fmoc group on the resin with 20% (v/v) 4-methylpiperidine/DMF. The resin was washed with DMF and proceeded to bromoacylation reaction with bromoacetic acid (0.8 M) and DIC (0.8 M) in DMF at room temperature for 20 min. The resin was washed with DMF and proceeded to the displacement reaction with amines at 1 M concentration in DMF at room temperature for 30 min. The resin was washed with DMF followed with dichloromethane (DCM), dried, and cleaved using 95% (v/v) TFA in water for 10 min at room temperature, followed by filtration and washing of the resin with DCM. The crude product was obtained by solvent evaporation using Biotage® V-10 evaporator and subsequent lyophilization from acetonitrile/water (1:1, v/v). Acetylation at the *N*-terminus of the crude peptoids (~200mg) was performed in 2 mL THF followed by the addition of acetic anhydride (100 µL) and pyridine (100 µL). The mixture was allowed to stir at room temperature for 1 h followed by solvent evaporation and lyophilization from acetonitrile/water (1:1, v/v).

The obtained crude peptoids were then purified by Waters reverse-phase HPLC on a XSelect HSS cyano column (5 µm, 18 × 150mm) using a linear, binary elution gradient (solvent A and B) from 50 to 95% B in 20 min at a flow rate of 15 mL/min. Here solvent A was 10% isopropanol in water, and solvent B was 10% isopropanol in acetonitrile. TFA was not added to the solvents considering the observed truncation of *N*-acetyl terminus under acidic conditions.[25] Collected HPLC fractions were analyzed by MALDI-TOF spectroscopy using α-cyano-4-hydroxycinnamic acid (CHCA) as the matrix, and reverse-phase analytical HPLC equipped with a cyano column and MicroTOF electrospray mass spectrometer. The pure fractions were combined followed by

solvent evaporation and lyophilization from acetonitrile/water (1:1, v/v) to afford a fluffy white powder.

Differential Scanning Calorimetry (DSC). All DSC measurements were performed on a TA Q200 differential scanning calorimeter. The dry white powder of peptoid (~2 mg) was added to a pre-weighed aluminum T Zero pan and sealed with an aluminum T Zero lid. The sample was treated with a heat-cool-heat cycle between 0-180 ^{o}C at a heating rate of 10 ^{o}C/min and a cooling rate of 5 ^{o}C/min.

Powder X-ray Diffraction (XRD). The peptoid samples (powder) were loaded onto MiteGen micromesh and heated in vacuum oven at 100^{o}C for 12h followed by slowly cooling down to room temperature. For the preparation of nanosheet samples, the nanosheet solutions were centrifuged at 13,200 rpm for 10 min and the resulting peptoid nanosheet pellets were pipetted onto MiteGen micromesh and dried under vacuum. Powder XRD measurements were performed at Advanced Light Source (ALS) beamline 8.3.1 located at Lawrence Berkeley National Laboratory. The beamline has a 5-tesla single pole superbend source (energy range 5-17 keV). The data were all collected with a 3 × 3 CCD array (ADSC Q315r) detector at a wavelength of 1.1159 Å. The distance of the detector from the sample was 350 mm. The diffraction patterns (Figure S16) were reduced using the Nika program for lgor Pro.

Self-Assembly of Diblock Copolypeptoids in Water. The purified peptoids was dissolved in THF/water mixed solvent (1/1, v/v) at a 2 mg/mL concentration. The mixture was placed, in an open container, at 4 ^{o}C refrigerator to slowly evaporate the THF. Cloudy solutions containing a large quantity of crystalline nanosheets were obtained after several days.

TEM Imaging of Nanosheets. TEM images of nanosheets were obtained from dry specimens. These specimens were prepared by drop casting a 3 μL droplet of the desired nanosheet-containing aqueous solution on a copper grid with the continuous carbon supporting film. The droplet was blotted from the edge of the grid using a filter paper. The micrographs were collected on a JEOL-1200 at 80 kV using a Gatan US1000 CCD camera at room temperature. The nanosheets were completely dry due to exposure to vacuum in the column of the TEM.

Atomic Force Microscopy (AFM) Imaging of Nanosheets. The AFM imaging of dry nanosheets was performed on Asylum MFP-3D atomic force microscope using tapping mode. The tips used in the study were TAP 150 AL-G tips with 150 kHz resonance frequency and 5 N/m force constant, respectively. The nanosheets solutions were diluted with milli-Q water and dropped onto freshly cleaved mica followed by drying under vacuum. *Ex situ* (in air) AFM imaging were performed for all the samples.

Results and Discussion

Design and Synthesis of Diblock Copolypeptoids. Amphiphilic diblock copolypeptoids, containing a hydrophilic block and a crystallizable hydrophobic block, are well known to phase separate and crystallize in bulk and in solution.[12, 19-20, 26] The solid-phase submonomer synthesis allows us to precisely tune not only the length and sequence, but also the overall molecular shape of the peptoid chain. In this study, a series of diblock copolypeptoids, bearing a hydrophilic poly(*N*-2-(2-methoxyethoxy)ethylglycine) (pNde) and a hydrophobic poly(*N*-alkylglycine), were designed and synthesized. The length of the pNde block was kept constant while the molecular shape of the hydrophobic poly(*N*-alkylglycine) block was varied. To alter the molecular shapes,

the side chain length was varied from *n*-hepyl to *n*-decyl, and their arrangements were manipulated to obtain three sets of diblock copolypeptoids with different molecular shapes (trapezoid, comb and zig-zag), as shown in Figure 1. All the peptoids were synthesized by solid-phase submonomer method and purified by reverse-phase high-performance liquid chromatography (HPLC) to >90% molecular purity. Detailed characterization data was included in the supporting information (Table S1 and Figures S1-S12.

Crystallization of Diblock Copolypeptoids in bulk. The crystallization behavior of all peptoids in bulk was investigated by both differential scanning calorimetry (DSC) and X-ray diffraction analyses. The DSC measurements were conducted in the temperature window between 0 and 180 ^{o}C and the thermograms of the second heating cycle are shown in Figure 2a. All the peptoids were crystallizable exhibiting a sharp thermal transition. It's intriguing that all the peptoids, regardless of their molecular shapes, showed a similar melting temperature in the temperature range of 80-84 ^{o}C. This suggests the likelihood that all the peptoids crystallize into a similar crystal lattice. To further explore the lattice structure, X-ray diffraction analyses were conducted for all the samples in bulk. As shown in Figure 2b and 2c, all the peptoids exhibited a nearly identical pattern of diffraction peaks, revealing a similar crystal lattice. The diffraction pattern observed was consistent with the known rectangular crystal lattice identified in our previously reported peptoid diblock copolymer systems.[19-20, 22] It should be noted that all the peptoids exhibited only one melting transition (T_m ~80 °C), whereas our earlier reported system with capped homo(*N*-alkylglycine) blocks showed two melting transitions corresponding to its liquid crystallinity[20]. Also, the XRD measurements of the peptoids in this study showed no discernible higher order peaks for (100) at ~4.6 Å, different than the capped homo(*N*-alkylglycine) system, where higher order peaks of (100) were clearly observed. These differences indicate that the

peptoids in this study have less ordered packing, probably owing to the hetero-length of side chains.

As a comparison, two peptoids in which the molecular shapes of the hydrophobic blocks are *not* self-complementary were also prepared (Figure S13). Interestingly, both peptoids can crystallize as evidenced by the melting transition in DSC measurements. However, their melting temperature is 5-10 °C lower as compared to peptoids **1-6** with self-complementary molecular shapes. As shown in Figure S13, the melting temperature decreased as the non-complementarity of the molecular shape increased, consistent with less ordered crystal packing in peptoids with non-complementary molecular shapes.

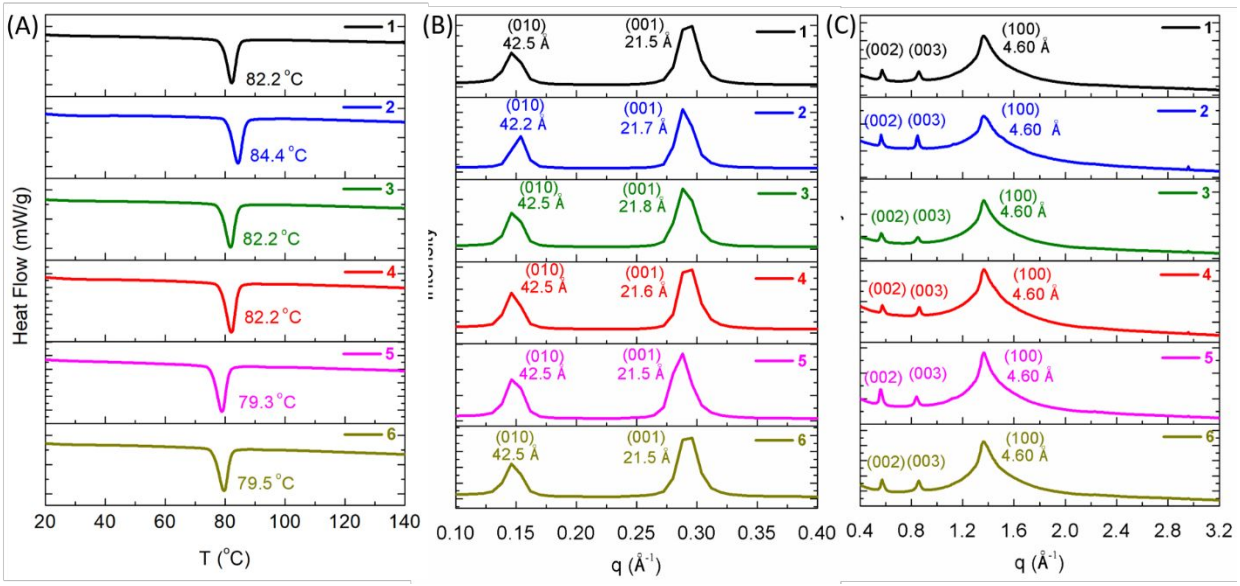

Figure 2. (A) DSC measurements of diblock copolyepeptoids **1-6** in bulk. (B, C) XRD measurements of diblock copolyepeptoids **1-6** in bulk with q range of 0.1-0.4 $Å^{-1}$ and 0.4-3.2 $Å^{-1}$, respectively.

Aqueous Self-assembly of Diblock Copolypeptoids. Amphiphilic diblock copolypeptoids have been shown to self-assemble in solution into various structures including spherical micelles[27],

nanosheets[22, 28-29], nanotubes[30-31], vesicles[32] and fibers[33]. The self-assembly behavior of all the diblock copolypeptoids in this study were investigated in water. The peptoids were dissolved in water/tetrahydrofuran (THF) (1:1 v/v) solution followed by evaporating the THF at 4 °C to drive the crystallization of the hydrophobic block. All the peptoids studied formed crystalline nanosheets in water, and the representative TEM and AFM images of sheet **1** were shown in Figures 3A-3C. NanoDSC analysis of the aqueous nanosheet solutions showed that they have a similar melting temperature in water, providing further evidence for their similar crystal packing (Figure S15). This likelihood was further supported by X-ray diffraction analyses of dry nanosheets showing a similar pattern of diffraction peaks as observed in the bulk materials (Figure 4). It should be noted that additional diffraction peaks at high q ranges, corresponding to higher order peaks of (100), were visible for sheet **1**, **2**, **3** and **4**. This suggested that these three sheets were more ordered than sheets **5** and **6** where the corresponding peaks were notably absent. The less ordered feature of sheet **5** and **6** is probably due to the zig-zag molecular shape of these two peptoids that makes the side chains more difficult to achieve perfect registry. The thickness of dry nanosheets measured by atomic force microscopy (AFM) was around 4.2 ± 0.3 nm (Figures 2C and 2D), which is in good agreement with the thickness obtained from the X-ray diffraction analysis (4.2 ± 0.2 nm).

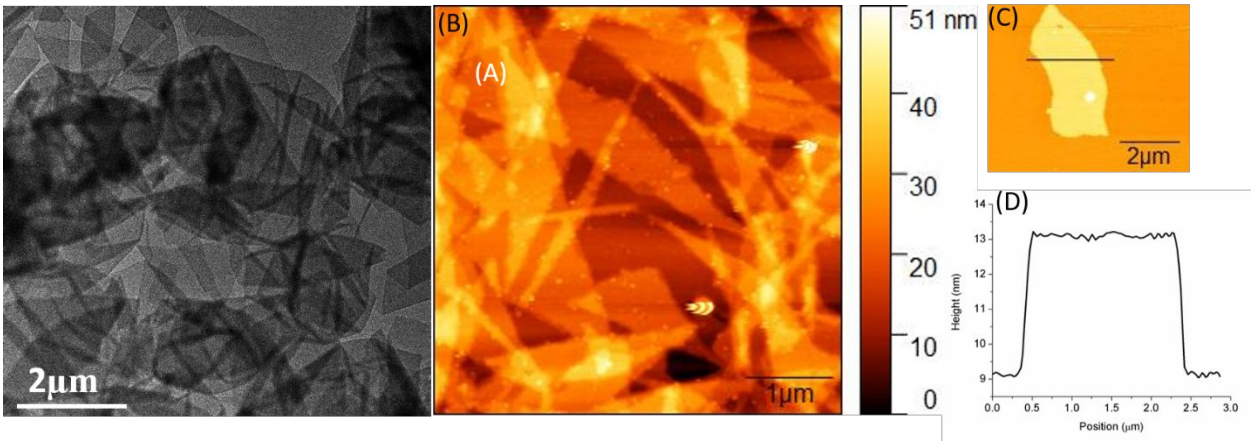

Figure 3. (A) Representative TEM image of sheet **1**. (B) Representative AFM image of sheet **1** using tapping mode. (C, D) Thickness profiles of sheet **1**.

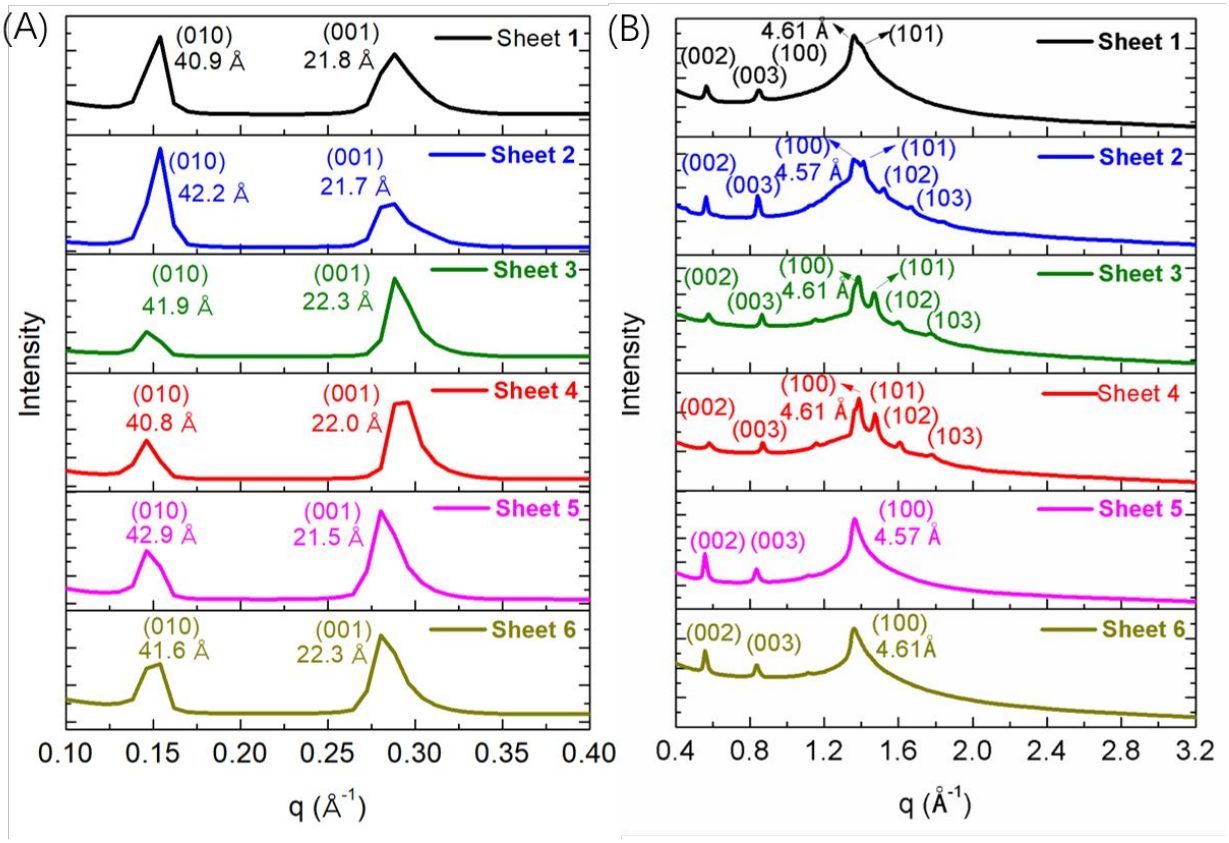

Figure 4. (A,B) XRD measurements of dry nanosheets **1-6** with q range of 0.1-0.4 $Å^{-1}$ and 0.4-3.2 $Å^{-1}$, respectively.

Proposed Molecular Packing Model of Nanosheets. Based on all the results mentioned above, we propose a nanosheet model in which the peptoid molecules are packed antiparallel along the *c* direction, and parallel along the *a* direction (Figure 5). In this way, the molecular shape of adjacent peptoid chains along the *c* direction is complementary to each other which allows them to pack into an ordered rectangular crystal lattice. For peptoids **3** and **4**, with an asymmetric pattern of alternating *n*-decyl and *n*-heptyl side chains, the decyl side chains are packed against heptyl side chains in the nanosheets, which is consistent with our earlier reported asymmetric

aromatic system.[22] It should also be noted that the *a* spacing (100) (~4.6 Å) of the crystal lattice, both in the bulk and the nanosheets, which is the distance between adjacent peptoid chains along the *a* direction, is in agreement with the universal spacing observed in other peptoid crystals.[19] The *b* spacing (010), which is the thickness of nanosheets, is consistent with that obtained from AFM measurements. The *c* spacing (001), which is the distance between adjacent backbones along the *c* direction, is dependent on the side chain length and fits well to the linear plot of *c* spacing with respect to side chain length in our previous study.[19]

These results show that the known crystal lattice of *N*-alkyl peptoids is further engineerable by changing the overall molecular shape of the hydrophobic domain. In contrast to previously reported *N*-alkyl peptoid crystals, where only one type of side chain was used in each hydrophobic block, the peptoids in this study had hetero-sequences with multiple distinct side chains in each hydrophobic block, and the rectangular crystal lattice was well-preserved. Additionally, this is different than the peptoids previously reported by Rosales *et al.* where point defects were precisely introduced into the crystal lattice[34], the peptoid crystals in the present study in effect contained no discernible defects, since the overall molecular shapes were designed to be self-complementary to enable inter-strand recognition.

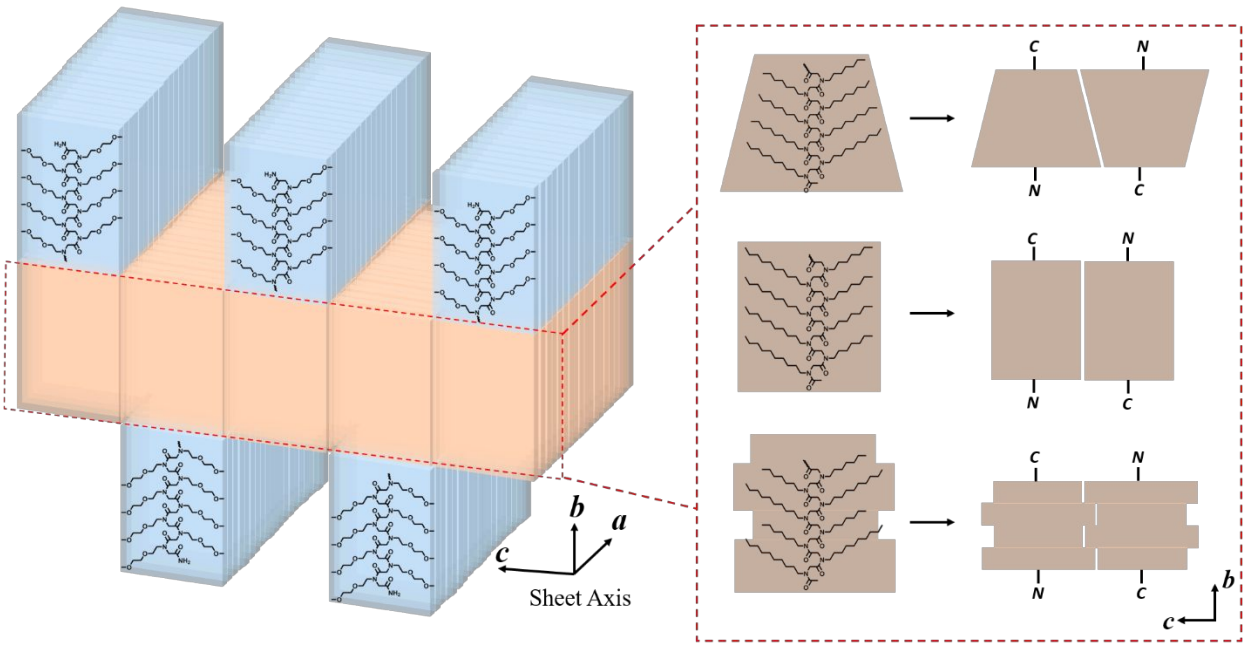

Figure 5. Proposed nanosheet models of amphiphilic diblock copolypeptoids: Polypeptoid chains are packed antiparallel along the *c* direction and parallel along the *a* direction. The hydrophobic block (orange color) is crystalline and the hydrophilic block (blue color) is amorphous[35]. The peptoids of different molecular shapes were packed into a similar rectangular crystal lattice, as shown in the red box. Labels "***C***" and "***N***" refer to the ***C***- and ***N***-terminus, respectively.

Conclusion

In this study, three sets of sequence-defined diblock copolypeptoids bearing different molecular shapes (trapezoid, comb and zig-zag) were designed and synthesized as a step to introduce features that enable a higher degree of inter-chain molecular recognition. We utilized their shape complementarity to achieve inter-strand recognized assembly between peptoid chains. Intriguingly, despite the varied molecular shapes, all the diblock copolypeptoids crystallized in

bulk into a similar rectangular crystal lattice, as revealed by their similar melting temperatures and X-ray diffraction patterns. All the peptoids also self-assembled into crystalline nanosheets in water with a similar rectangular crystal lattice as that observed in the bulk material, regardless of their different molecular shapes. These results inspire us to further explore the degree of specificity of these peptoids in co-assembly experiments in bulk or solution, to determine whether the peptoids can segregate into separate lattices. This work sets the stage to exploit small differences in shape to achieve selectivity in bulk and solution assembly. The inter-strand recognition of these peptoids also inspires us to design two distinct peptoid strands that are not self-complementary, yet can co-assemble to segregate into alternating rows in an antiparallel manner in solution. In this way, Janus peptoid nanosheets with different functionalities on the two surfaces could be potentially created, which is of great interest in both material sciences and biotechnology. These investigations are currently underway. These results suggest that the molecular shape complementarity could be a potential design element for the construction of more complicated peptoid nanomaterials that rival the structural and functional complexity found in nature.

Conflicts of interest

There are no conflicts to declare.

Author information

Corresponding author

* rnzuckermann@lbl.gov

Acknowledgements

Primary funding for this work was provided by the Soft Matter Electron Microscopy Program (KC11BN), supported by the Office of Science, Office of Basic Energy Science, US Department of Energy, under Contract DE-AC02-05CH11231. Work at the Molecular Foundry and the Advanced Light Source at Lawrence Berkeley National Laboratory was supported by user projects at these user facilities, supported by the Office of Science, Office of Basic Energy Sciences, of the US Department of Energy under Contract DE-AC02-05CH11231. Micrographs presented here were obtained at the Donner Cryo-TEM facility in Lawrence Berkeley National Laboratory and the Berkeley Bay Area Cryo-TEM facility at the University of California, Berkeley. We thank George Meigs for their assistance with the XRD measurements.

References

1. Watson, J. D.; Crick, F. H. C., Genetical Implications of the Structure of Deoxyribonucleic Acid. *Nature* **1953,** *171* (4361), 964-967.
2. Gong, B., Molecular Duplexes with Encoded Sequences and Stabilities. *Acc. Chem. Res.* **2012,** *45* (12), 2077-2087.
3. Lee, S.-H.; Ouchi, M.; Sawamoto, M., Supramolecular X-Shaped Homopolymers and Block Polymers by Midsegment Complementary Hydrogen Bonds: Design of Bifunctional Initiators with Interactive Sites for Metal-Catalyzed Living Radical Polymerization. *Macromolecules* **2012,** *45* (9), 3702-3710.
4. Zhu, Y.; Hu, J.; Liu, Y., Shape memory effect of thermoplastic segmented polyurethanes with self-complementary quadruple hydrogen bonding in soft segments. *The European Physical Journal E* **2009,** *28* (1), 3-10.
5. Jones, S.; Thornton, J. M., Principles of protein-protein interactions. *Proc. Natl. Acad. Sci.* **1996,** *93* (1), 13-20.
6. Kortagere, S.; Krasowski, M. D.; Ekins, S., The importance of discerning shape in molecular pharmacology. *Trends Pharmacol. Sci.* **2009,** *30* (3), 138-147.
7. Gerling, T.; Wagenbauer, K. F.; Neuner, A. M.; Dietz, H., Dynamic DNA devices and assemblies formed by shape-complementary, non–base pairing 3D components. *Science* **2015,** *347* (6229), 1446-1452.
8. Hwang, W.; Yoo, J.; Hwang, I.-C.; Lee, J.; Ko, Y. H.; Kim, H. W.; Kim, Y.; Lee, Y.; Hur, M. Y.; Park, K. M.; Seo, J.; Baek, K.; Kim, K., Hierarchical Self-Assembly of Poly-Pseudorotaxanes into Artificial Microtubules. *Angew. Chem. Int. Ed.* **2020,** *59* (9), 3460-3464.

9. Li, N.; Wu, F.; Han, Z.; Wang, X.; Liu, Y.; Yi, C.; Ye, S.; Lu, G.; Yu, L.; Nie, Z.; Ding, B., Shape Complementarity Modulated Self-Assembly of Nanoring and Nanosphere Hetero-nanostructures. *J. Am. Chem. Soc.* **2020,** *142* (27), 11680-11684.
10. Sacanna, S.; Korpics, M.; Rodriguez, K.; Colón-Meléndez, L.; Kim, S.-H.; Pine, D. J.; Yi, G.-R., Shaping colloids for self-assembly. *Nat. Commun.* **2013,** *4* (1), 1688.
11. Paik, T.; Murray, C. B., Shape-Directed Binary Assembly of Anisotropic Nanoplates: A Nanocrystal Puzzle with Shape-Complementary Building Blocks. *Nano Lett.* **2013,** *13* (6), 2952-2956.
12. Xuan, S.; Zuckermann, R. N., Diblock copolypeptoids: a review of phase separation, crystallization, self-assembly and biological applications. *J. Mater. Chem. B* **2020,** *8* (25), 5380-5394.
13. Xuan, S.; Zuckermann, R. N., Engineering the atomic structure of sequence-defined peptoid polymers and their assemblies. *Polymer* **2020,** *202*, 122691.
14. Battigelli, A., Design and preparation of organic nanomaterials using self-assembled peptoids. *Biopolymers* **2019,** *110* (4), e23265.
15. Robertson, E. J.; Battigelli, A.; Proulx, C.; Mannige, R. V.; Haxton, T. K.; Yun, L.; Whitelam, S.; Zuckermann, R. N., Design, Synthesis, Assembly, and Engineering of Peptoid Nanosheets. *Acc. Chem. Res.* **2016,** *49* (3), 379-389.
16. Zuckermann, R. N.; Kerr, J. M.; Kent, S. B. H.; Moos, W. H., Efficient method for the preparation of peptoids [oligo(N-substituted glycines)] by submonomer solid-phase synthesis. *J. Am. Chem. Soc.* **1992,** *114* (26), 10646-10647.
17. Leguizamon, S. C.; Scott, T. F., Sequence-selective dynamic covalent assembly of information-bearing oligomers. *Nat. Commun.* **2020,** *11* (1), 784.
18. Leguizamon, S. C.; Alqubati, A. F.; Scott, T. F., Temperature-mediated molecular ladder self-assembly employing Diels–Alder cycloaddition. *Polym. Chem.* **2020,** *11* (48), 7714-7720.
19. Greer, D. R.; Stolberg, M. A.; Kundu, J.; Spencer, R. K.; Pascal, T.; Prendergast, D.; Balsara, N. P.; Zuckermann, R. N., Universal Relationship between Molecular Structure and Crystal Structure in Peptoid Polymers and Prevalence of the cis Backbone Conformation. *J. Am. Chem. Soc.* **2018,** *140* (2), 827-833.
20. Greer, D. R.; Stolberg, M. A.; Xuan, S.; Jiang, X.; Balsara, N. P.; Zuckermann, R. N., Liquid-Crystalline Phase Behavior in Polypeptoid Diblock Copolymers. *Macromolecules* **2018,** *51* (23), 9519-9525.
21. Pierri, G.; Schettini, R.; Nuss, J.; Dinnebier, R. E.; De Riccardis, F.; Izzo, I.; Tedesco, C., Cyclic hexapeptoids with N-alkyl side chains: solid-state assembly and thermal behaviour. *CrystEngComm* **2020,** *22* (38), 6371-6384.
22. Xuan, S.; Jiang, X.; Spencer, R. K.; Li, N. K.; Prendergast, D.; Balsara, N. P.; Zuckermann, R. N., Atomic-level engineering and imaging of polypeptoid crystal lattices. *Proc. Natl. Acad. Sci.* **2019,** *116* (45), 22491-22499.
23. Jiang, X.; Greer, D. R.; Kundu, J.; Ophus, C.; Minor, A. M.; Prendergast, D.; Zuckermann, R. N.; Balsara, N. P.; Downing, K. H., Imaging Unstained Synthetic Polymer Crystals and Defects on Atomic Length Scales Using Cryogenic Electron Microscopy. *Macromolecules* **2018,** *51* (19), 7794-7799.
24. Jiang, X.; Xuan, S.; Kundu, J.; Prendergast, D.; Zuckermann, R. N.; Balsara, N. P., Effect of processing and end groups on the crystal structure of polypeptoids studied by cryogenic electron microscopy at atomic length scales. *Soft Matter* **2019,** *15* (23), 4723-4736.
25. Kim, S.; Biswas, G.; Park, S.; Kim, A.; Park, H.; Park, E.; Kim, J.; Kwon, Y.-U., Unusual truncation of N-acylated peptoids under acidic conditions. *Org. Biomol. Chem.* **2014,** *12* (28), 5222-5226.
26. Sun, J.; Teran, A. A.; Liao, X.; Balsara, N. P.; Zuckermann, R. N., Crystallization in Sequence-Defined Peptoid Diblock Copolymers Induced by Microphase Separation. *J. Am. Chem. Soc.* **2014,** *136* (5), 2070-2077.

27. Sternhagen, G. L.; Gupta, S.; Zhang, Y.; John, V.; Schneider, G. J.; Zhang, D., Solution Self-Assemblies of Sequence-Defined Ionic Peptoid Block Copolymers. *J. Am. Chem. Soc.* **2018,** *140* (11), 4100-4109.
28. Jin, H.; Jiao, F.; Daily, M. D.; Chen, Y.; Yan, F.; Ding, Y.-H.; Zhang, X.; Robertson, E. J.; Baer, M. D.; Chen, C.-L., Highly stable and self-repairing membrane-mimetic 2D nanomaterials assembled from lipid-like peptoids. **2016,** *7*, 12252.
29. Shi, Z.; Wei, Y.; Zhu, C.; Sun, J.; Li, Z., Crystallization-Driven Two-Dimensional Nanosheet from Hierarchical Self-Assembly of Polypeptoid-Based Diblock Copolymers. *Macromolecules* **2018,** *51* (16), 6344-6351.
30. Jin, H.; Ding, Y.-H.; Wang, M.; Song, Y.; Liao, Z.; Newcomb, C. J.; Wu, X.; Tang, X.-Q.; Li, Z.; Lin, Y.; Yan, F.; Jian, T.; Mu, P.; Chen, C.-L., Designable and dynamic single-walled stiff nanotubes assembled from sequence-defined peptoids. *Nat. Commun.* **2018,** *9* (1), 270.
31. Sun, J.; Jiang, X.; Lund, R.; Downing, K. H.; Balsara, N. P.; Zuckermann, R. N., Self-assembly of crystalline nanotubes from monodisperse amphiphilic diblock copolypeptoid tiles. *Proc. Natl. Acad. Sci.* **2016,** *113* (15), 3954-3959.
32. Deng, Y.; Chen, H.; Tao, X.; Cao, F.; Trépout, S.; Ling, J.; Li, M.-H., Oxidation-Sensitive Polymersomes Based on Amphiphilic Diblock Copolypeptoids. *Biomacromolecules* **2019,** *20* (9), 3435-3444.
33. Lee, C.-U.; Smart, T. P.; Guo, L.; Epps, T. H.; Zhang, D., Synthesis and Characterization of Amphiphilic Cyclic Diblock Copolypeptoids from N-Heterocyclic Carbene-Mediated Zwitterionic Polymerization of N-Substituted N-Carboxyanhydride. *Macromolecules* **2011,** *44* (24), 9574-9585.
34. Rosales, A. M.; Murnen, H. K.; Zuckermann, R. N.; Segalman, R. A., Control of Crystallization and Melting Behavior in Sequence Specific Polypeptoids. *Macromolecules* **2010,** *43* (13), 5627-5636.
35. Sun, J.; Stone, G. M.; Balsara, N. P.; Zuckermann, R. N., Structure–Conductivity Relationship for Peptoid-Based PEO–Mimetic Polymer Electrolytes. *Macromolecules* **2012,** *45* (12), 5151-5156.